Intense Focused Ultrasound: Evaluation of a New Treatment Modality for Precise Microcoagulation within the Skin

Hans J. Laubach, MD,* Inder R. S. Makin, MD, PhD,† Peter G. Barthe, PhD,† Michael H. Slayton, PhD,† and Dieter Manstein, MD*

BACKGROUND AND OBJECTIVE Focused ultrasound can produce thermal and/or mechanical effects deep within tissue. We investigated the capability of intense focused ultrasound to induce precise and predictable subepidermal thermal damage in human skin.

MATERIALS AND METHODS Postmortem human skin samples were exposed to a range of focused ultrasound pulses, using a prototype device (Ulthera Inc.) emitting up to 45 W at 7.5 MHz with a nominal focal distance of 4.2 mm from the transducer membrane. Exposure pulse duration ranged from 50 to 200 ms. Thermal damage was confirmed by light microscopy using a nitroblue tetrazolium chloride assay, as well as by loss of collagen birefringence in frozen sections. Results were compared with a computational model of intense ultrasound propagation and heating in tissue.

RESULTS Depth and extent of thermal damage were determined by treatment exposure parameters (source power, exposure time, and focal depth). It was possible to create individual and highly confined lesions or thermal damage up to a depth of 4 mm within the dermis. Thermal lesions typically had an inverted cone shape. A precise pattern of individual lesions was achieved in the deep dermis by applying the probe sequentially at different exposure locations.

DISCUSSION AND CONCLUSION Intense focused ultrasound can be used as a noninvasive method for spatially confined heating and coagulation within the skin or its underlying structures. These findings have a significant potential for the development of novel, noninvasive treatment devices in dermatology.

Ulthera Inc. provided the prototype intense ultrasound device for this study. Inder Makin, Peter Barthe, and Michael Slayton are employees of Ulthera.

Laser- and light-based devices have been introduced during the past years for noninvasive heating of the dermis without epidermal damage.[1–4] Epidermal protection is achieved by skin surface cooling during exposure, creating an inverse temperature gradient within the skin. While optical beams can be superficially focused, photon scattering prevents deep focusing of light within the skin.

High-intensity focused ultrasound (HIFU) has been investigated as a tool for the treatment of solid benign and malignant tumors for many decades, but is only now beginning to emerge as a potential noninvasive alternative to conventional therapies.[5–20] The histologic morphology of tissue destruction induced by focused ultrasound (US) shows coagulative necrosis with precisely defined, sharp margins to normal tissue.[21] The primary physical mechanism responsible for tissue necrosis with focused US treatment is heating due to absorption of acoustic energy, although some concomitant inertial cavitational response of tissue from an intense US field is probably also present.[22–25] The US beam increases the tissue temperature within a focal volume to the point at which a wide spectrum of tissue modification can take place. The spectrum of cellular changes depends on temperature rise and exposure duration and range from necrosis to more subtle ultrastructural cell damage with modulation of cellular cytokine expression.[26] These findings are similar to the thermally induced changes within the skin after ablative and nonablative laser or light treatments.[3,27]

*Wellman Center for Photomedicine, Massachusetts General Hospital, Harvard Medical School, Boston, Massachusetts; †Ulthera Inc., Mesa, Arizona

 • Published by Blackwell Publishing •
ISSN: 1076-0512 • Dermatol Surg 2008;34:727–734 • DOI: 10.1111/j.1524-4725.2008.34196.x

The classic HIFU applications described in the scientific literature relate primarily to the delivery of a high-powered focused US field to "debulk" tissue. The sources characteristically deposit (focus) acoustic energy at a location distal to the source plane over a period of seconds, whereby a region of tissue necrosis is achieved. This process is repeated over a significant volume of tissue (typically several cubic centimeters), to achieve thermal destruction of the entire target pathology. These HIFU procedures typically take between 30 and 180 minutes to complete[6,17,28] depending on the target volume of treatment. In contrast to the traditional HIFU treatment, the US approach described in this study deposits short pulses of intense focused ultrasound (IFUS) in the millisecond domain (50–200 ms). Avoiding cavitational processes, a frequency in the megahertz (MHz) domain is used instead of the kilohertz (KHz) domain frequencies as commonly utilized in HIFU. The nominal energy level deposited at each site with this approach is also significantly lower (0.5–10 J) compared to HIFU (100 J). The goal of this study is to investigate the ability of this US therapy approach to noninvasively induce precise thermal damage in human skin.

Materials and Methods

Intense US Prototype Device

Experiments were performed in vitro, on postmortem human skin samples with a custom-developed IFUS prototype device (Ulthera Inc., Mesa, AZ). An US probe is connected to a generator system operating in the MHz frequency regime. The US energy is coupled from the transducer (operating at 7.5 MHz) to skin tissue by ultrasound coupling gel applied to the skin surface. The nominal focal depth for this study was 4.2 mm below the skin surface (Ulthera Inc.).

Tissue Samples and Tissue Processing

For the in vitro evaluation we used cryopreserved (−80°C), full-thickness skin samples of different body sites and a Fitzpatrick Skin Type II to V. Dermal thickness of tissue samples ranged from 2 to 5 mm and total thickness including subcutaneous tissue was up to 20 mm. Tissue samples were defrosted from −80°C, and care was taken that the entire tissue sample was heated to 35°C. After exposure, tissue was again frozen immediately to −80°C and processed by frozen sectioning in the upcoming days. After the exposure, tissue specimens were processed for frozen sections. Cross-sections of 10 μm thickness were collected every 200 μm for further processing and histologic evaluation. This approach allowed for a three-dimensional understanding of the histology of the treated zone. Thermal damage patterns in the tissue were assessed for microscopic evaluations with a nitroblue tetrazolium chloride (NBTC) assay for cell viability as described by Neumann and coworkers.[29] Furthermore, tissue sections for histologic evaluation were counterstained with eosin to increase contrast and show possible collagen denaturation. Cross-polarized light was also used to confirm collagen denaturation by loss of birefringence.

US Exposures

Exposures were performed in vitro on postmortem human skin samples at tissue temperatures of 35°C. The temperature of skin sample was kept constant by a heating plate on which the sample was placed and monitored before exposures with a contact thermometer. The prototype probe was acoustically coupled to the human skin sample, using US coupling gel. Single exposures were performed at set power levels and exposure durations. Exposure duration was varied from 50 to 200 ms, output power was set to a maximum of 45 W, and no active cooling was used before, during, or after the exposure. Exposure locations were then marked and sectioned for further histologic evaluation.

Numerical Simulations

The propagation of the focused US beam in skin tissue was modeled using an approach described by Hasegawa and coworkers.[30] The acoustic field simulation accounts for the geometric focusing as well as the attenuation of energy in the epidermis, dermis, and hypodermis. The thermal gradients

resulting from absorption of acoustic energy in tissue and conversion to heat were calculated using the Bioheat equation.[31] The $>60^{\circ}$C contours indicating complete collagen disruption were chosen to represent the zone of thermal injury.[23,31,32]

Results

Exposure durations of 150 ms and above resulted in a palpable and macroscopically visible intracutaneous nodule of approximately 1-mm diameter. The skin surface was slightly raised over US-induced dermal nodules but did not show any evident blister. Exposure durations of 125 ms and below could not be detected by clinical examination (observation and palpation) of the skin samples. Histologic evaluation by both NBTC and standard H&E-stained light microscopy showed that intradermal lesions created by the single US exposure pulses in this study, although different in size, were typically inverted cone–shaped. Thermal lesions consisted of a core defined by an area of thermal cell necrosis and collagen denaturation as determined by the loss of NBTC staining and loss of birefringence, respectively (Figures 2A, 3A, and 3B). The lesions typically begin in the deep reticular dermis at a depth of approximately 3 to 4 mm (Figure 2A). Serial steps sectioning as described under Materials and Methods through the entire skin samples did not detect any epidermal damage. Increasing the exposure time and energy delivered caused the thermal lesions to extend from the deeper reticular dermis toward the papillary dermis. At exposure durations of 175 ms and above, the lesions consisted of overt damage of the entire dermal thickness and overlying epidermis (Figure 1A). A single US exposure of 50 ms produced well-confined thermal lesions with NBTC staining loss of approximately 200×300 µm at a depth of 2.7 mm deep within the reticular dermis (Figures 3A and 3B). Figure 4 shows the result of multiple exposures within one skin sample of Fitzpatrick Skin Type V. Lesions can be placed independently from each other without confluent damage. If the dermal thickness is less than the focal depth of the intense US device, thermal lesions are placed within the underlying

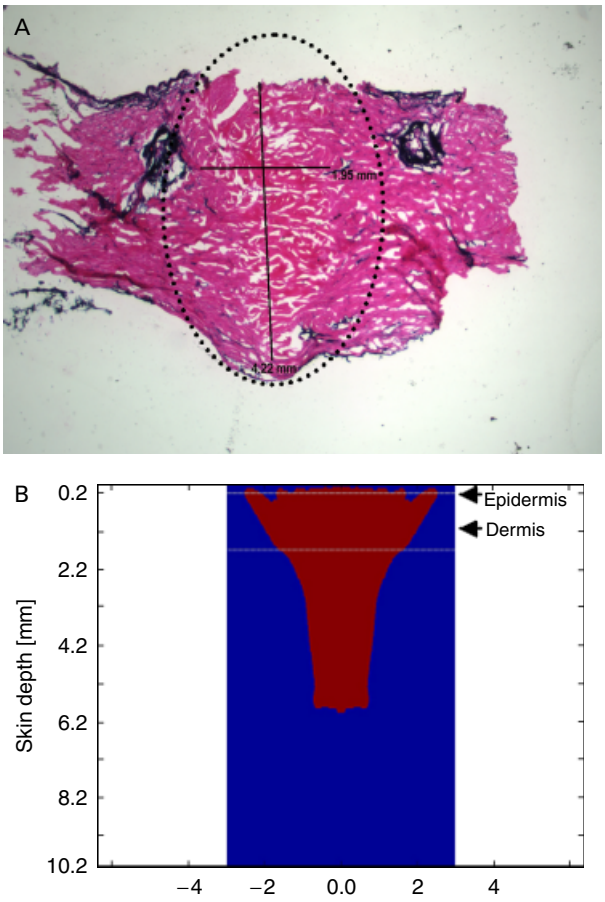

Figure 1. (A) NBTC assay with eosin counterstain; × 12.5 magnification; single US exposure, 45 W, 200-ms pulse duration, 7.5 MHz, 4.2-mm focal depth. Complete loss of NBTC staining and collagen denaturation throughout the entire dermis (black circle). Please note the artifact due to tissue preparation with loss of epidermal tissue in necrotic zone due to the thermal alteration of tissue integrity and resulting friability. (B) Numerical simulation of the thermal response of skin to source conditions corresponding to the experimental results in A. The zone of thermal coagulation in this simulation is represented by the 60°C temperature contour in the skin tissue.

structures, e.g., subcutaneous adipose tissue. The theoretical size and location of thermal lesions predicted from numerical simulations compared well with the observed experimental zone of thermal coagulation (see Figures 1–4). The computationally predicted lesions in these results are nominally longer axially, compared to the experimentally observed thermal lesions. This discrepancy is most likely due to the fact that the simulations do not account for the change in tissue properties subsequent to the change of temperature.[23,34]

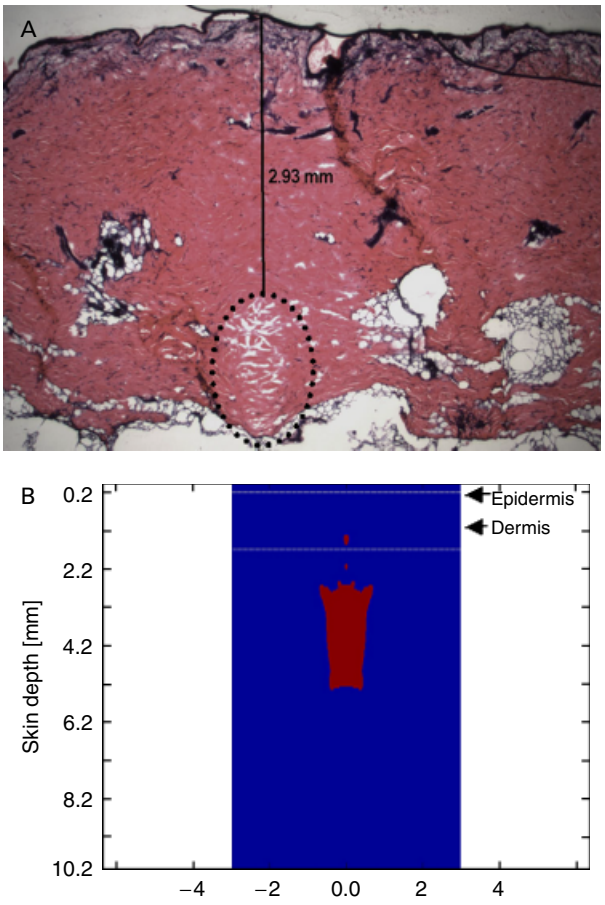

Figure 2. (A) NBTC assay with eosin counterstain; × 12.5 magnification; single US exposure, 45 W, 75-ms pulse duration, 7.5 MHz, 4.2-mm focal depth. Well-confined zone of thermal damage within the dermis (black circle). (B) Numerical simulation of the thermal response of skin tissue to source conditions corresponding to the experimental results in A. The zone of thermal coagulation in this simulation is represented by the 60°C temperature contour in the skin tissue.

Discussion

Classic HIFU treatment is using the concept of thermal tissue injury due to the absorption of US energy.[35–37] It has been investigated as a noninvasive treatment modality tool for benign and malignant tumors for many decades and has now been applied as a noninvasive alternative to conventional therapies for nearly a decade.[13,24,38,39] Van Leenders and colleagues,[26] for example, have shown that it is possible to thermally confine an US-induced thermal treatment zone within the prostate gland. This allowed HIFU to become one of clinical treatment alternatives in the treatment of benign prostatic hyperplasia and prostate cancer.[5–8,40] While HIFU can been used to thermally ablate tissue on a macroscopic scale (in the range of several cubic centimeters),[25,26,41] we investigated in this study the potential for focused US as a treatment modality to induce micro-thermal tissue denaturation within the human skin. As demonstrated by the numerical simulation results and confirmed by the characteristic coagulative change shown in the histology from our study, the US treatment regime (e.g., frequency, power and exposure duration) caused well-defined zones of thermal injury within the dermis. Figures 2–4 show those confined zones of microscopic tissue ablation induced by focused US using relatively high acoustic intensity delivered within milliseconds. Owing to the relatively short exposure duration as well as the sharp focusing, it is possible to deliver US energy at significantly lower energies than classic HIFU to achieve a microscopically small volume of thermally ablated tissue ($<1\,mm^3$). Compared to classic HIFU, exposure durations used are significantly lower (in the millisecond domain), the total energy delivered per pulse is considerably smaller (below 15 J/pulse), and the focal spot within the skin achieves a zone of thermal tissue effect on the order of $1\,mm^3$ and smaller. By choosing the appropriate exposure parameters with the IFUS approach, we were able to spare the epidermis as well as avoid damage to the papillary dermis without simultaneous skin cooling, while creating a zone of thermal coagulation deep within the reticular dermis (Figures 2 and 3). With increase in the exposure time, the thermal lesion grows typically in its axial dimension, progressing proximally toward the skin surface (Figure 1) while shorter exposure times not only decrease the lesion size (Figures 2 and 3) but also minimize the risk of uncontrolled bulk heating and thermal diffusion into adjacent tissue. Chen and coworkers[42] reported that typically cigar-shaped lesions are observed in tissue phantoms after HIFU exposure. These lesions take a tadpolelike appearance once boiling temperatures are reached. We observed similarly shaped lesions within the dermis in our study (Figure 2). The lesions were typically cigar- or inverted cone–shaped and started in the lower

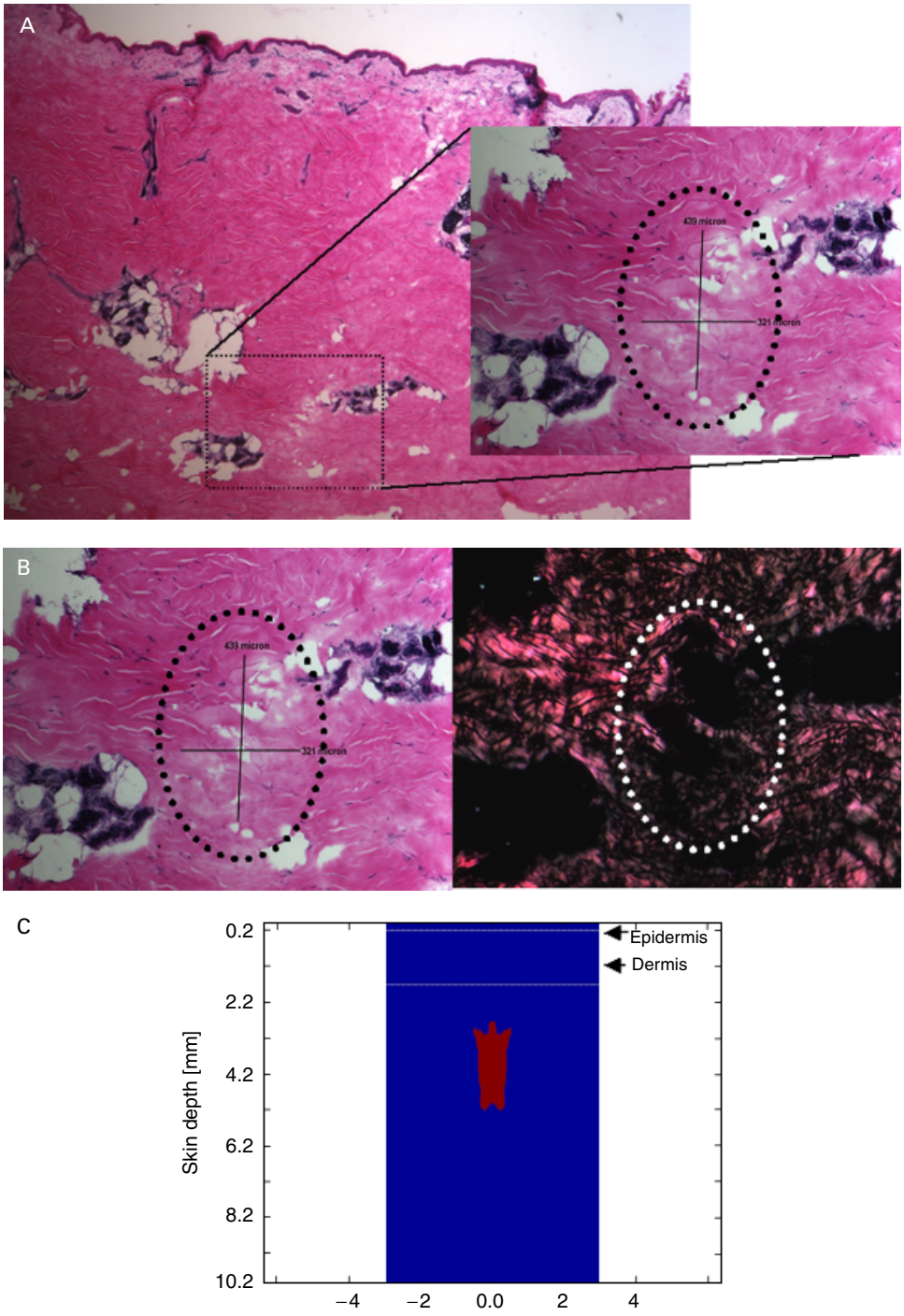

Figure 3. (A) NBTC assay with eosin counterstain; × 12.5 and × 100 magnification; single US exposure, 45 W, 50-ms pulse duration, 7.5 MHz, 4.2-mm focal depth. Small and well-confined thermal lesion deep within the deep reticular dermis (black circle). (B) Same × 100 magnification close up as in A with corresponding cross-polarized image showing complete loss of birefringence in thermal damage zone (white circle). (C) Numerical simulation of the thermal response of skin tissue to source conditions corresponding to the experimental results in A. The zone of thermal coagulation in this simulation is represented by the 60°C temperature contour in the skin tissue.

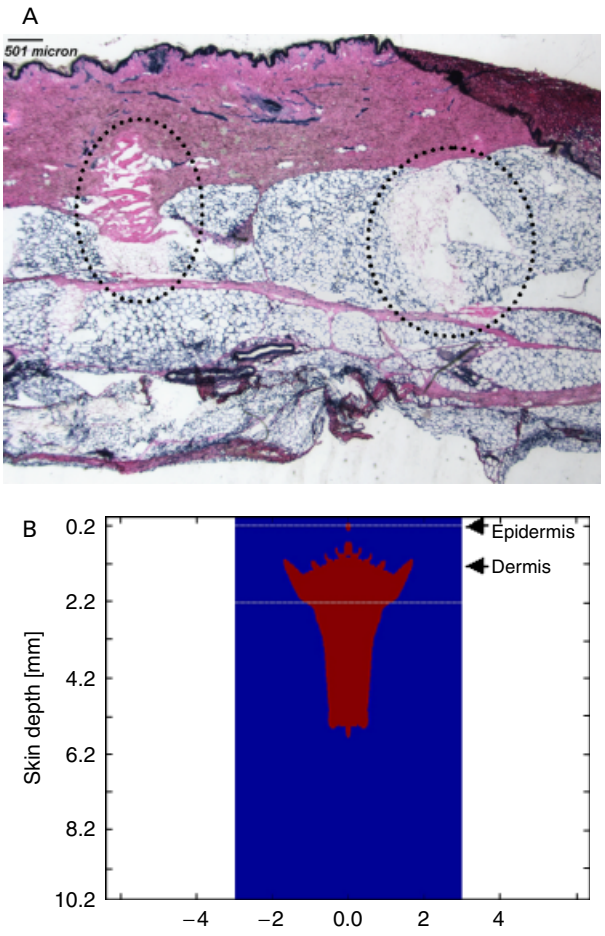

Figure 4. (A) NBTC assay with eosin counterstain, × 12.5 magnification, two separate US pulses deposited 3 mm apart, 45 W, 125-ms pulse duration, 7.5 MHz, 4.2-mm focal depth. Two spatially distinct zones of thermal damage within the dermis and the subcutaneous fat (black circles). Please note that the dermis of this skin sample is thinner than that in Figures 1–3. Therefore, a focal depth of 4.2 mm places the thermal damage zones within the subdermal tissue. (B) Numerical simulation of the thermal response of skin tissue to source conditions corresponding to the experimental results in A. The zone of thermal coagulation in this simulation is represented by the 60°C temperature contour in the skin tissue.

reticular dermis. It is noteworthy that the thermal lesions on histologic analysis were found slightly above the geometric focus as predicted by the beam geometry and the computer simulation. One possible explanation for this observation can be found in Bush and colleagues,[43] who described that when tissue heating occurs, the attenuation within that volume increases, altering the absorbed energy distribution. The region in which heat is deposited is expected to alter its absorption properties during the heating process, thereby shifting the region of intensity maximum toward the transducer.[44,45] Since the tissue properties change dynamically as US energy is deposited, future studies should more extensively investigate multiple lesion formation and variability of response at fixed source conditions. Another difference between classic HIFU treatments and IFUS is that in the clinical setting of HIFU therapy convective and conductive energy losses play an important role since exposure durations are in the order of seconds and longer. Owing to the short exposure durations (on the order of several milliseconds), the coagulative tissue effect with IFUS is mostly independent of these losses and is also not accounted for in our numerical modeling.

Comparing the outline of the lesion determined by loss of collagen birefringence in comparison with the loss of NBTC staining behavior has been examined, and a small size difference could be observed. The lesion as determined by loss of collagen birefringence appeared to be consistently smaller than the lesion determined by loss of NBTC stain. To determine the exact difference in between these two lesions, although interesting, is out of the scope of this study. One inherent advantage of the noninvasive therapy with US compared to light-based devices is its independence of chromophores for energy absorption. As demonstrated in Figure 4, even a skin sample with Fitzpatrick Skin Type V was treated, and well-defined lesions could be created within the deeper dermis and the subcutaneous tissue without simultaneous skin cooling. No damage is observed in the upper dermis and the overlying epidermis. The advantage for the dermatologic use of IFUS is that the absorption of US energy is independent of the melanin content of skin. Its absorption is rather determined by the microscopic and bulk mechanical properties of tissue.[37,46] Therefore, in contrast to light-based devices, the action of IFUS is independent of skin color and chromophores. The "colorblind" IFUS treatment approach might be helpful in overcoming some of the difficulties encountered with the light-based treatment of darker skin types. In addition

to its independence of chromophores, IFUS creates a sharp focus of the US beam several millimeters within the skin. Hence the power density of the converging US beam is much lower as it passes through epidermis than in its focal point. Therefore, only minimal energy absorption and tissue heating occurs at the epidermal level insufficient to create significant thermal damage. This consequently obviates the need for skin cooling for epidermal protection for any skin type as it is used with other devices inducing unexpected thermal alterations within the skin.

As demonstrated in Figure 4, several separate lesions can be placed next to each other within the skin using IFUS. This allows for the creation of a number of unique thermal damage patterns. Tissue may be altered by arrays of microscopically small focal damage from IFUS rather than ablating an entire macroscopic area allowing a rapid healing response from tissue immediately adjacent to the thermal lesions, conceptually similar to laser fractional photothermolysis.[47] It remains furthermore to be determined in how far US "see-and-treat" systems, as they are already established for HIFU therapy,[40,48] can also be used for the guidance and monitoring of IFUS in the dermatologic use.

Intense focused ultrasound provides the possibility to thermally coagulate a target deep within the skin or below without affecting the intervening tissue. Compared to similar nonablative therapies based on light or radiofrequency, IFUS has the capability of precisely controlling the amount and location of thermal injury at a known depth below the skin surface. IFUS is a new treatment modality, offering the potential for novel, noninvasive treatment concepts in dermatology.

Conclusion

Intense focused ultrasound can be used as a noninvasive method for spatially confined heating and coagulation within the skin or its underlying structures.

Acknowledgments The authors thank Qiqi Mu, MD, for her support with tissue sectioning and Bill Farinelli for his unceasing technical succor.

References

1. Goldberg DJ, Whitworth J. Laser skin resurfacing with the Q-switched Nd:YAG laser. Dermatol Surg 1997;23:903; discussion 906–7.
2. Herne KB, Zachary CB. New facial rejuvenation techniques. Semin Cutan Med Surg 2000;19:221–31.
3. Menaker GM, Wrone DA, Williams RM, Moy RL. Treatment of facial rhytids with a nonablative laser: a clinical and histologic study. Dermatol Surg 1999;25:440–4.
4. Dierickx CC. The role of deep heating for noninvasive skin rejuvenation. Lasers Surg Med 2006;38:799–807.
5. Chapelon JY, Ribault M, Vernier F, et al. Treatment of localised prostate cancer with transrectal high intensity focused ultrasound. Eur J Ultrasound 1999;9:31–8.
6. Foster RS, Bihrle R, Sanghvi NT, et al. High-intensity focused ultrasound in the treatment of prostatic disease. Eur Urol 1993;23(Suppl 1):29–33.
7. Gelet A, Chapelon JY, Bouvier R, et al. Local control of prostate cancer by transrectal high intensity focused ultrasound therapy: preliminary results. J Urol 1999;161:156–62.
8. Gelet A, Chapelon JY, Bouvier R, et al. Treatment of prostate cancer with transrectal focused ultrasound: early clinical experience. Eur Urol 1996;29:174–83.
9. Gianfelice D, Khiat A, Amara M, et al. MR imaging-guided focused ultrasound surgery of breast cancer: correlation of dynamic contrast-enhanced MRI with histopathologic findings. Breast Cancer Res Treat 2003;82:93–101.
10. Gianfelice D, Khiat A, Amara M, et al. MR imaging-guided focused US ablation of breast cancer: histopathologic assessment of effectiveness—initial experience. Radiology 2003;227: 849–55.
11. Gianfelice D, Khiat A, Boulanger Y, et al. Feasibility of magnetic resonance imaging-guided focused ultrasound surgery as an adjunct to tamoxifen therapy in high-risk surgical patients with breast carcinoma. J Vasc Interv Radiol 2003;14: 1275–82.
12. Harari PM, Hynynen KH, Roemer RB, et al. Development of scanned focussed ultrasound hyperthermia: clinical response evaluation. Int J Radiat Oncol Biol Phys 1991;21:831–40.
13. Hill CR, ter Haar GR. Review article: high intensity focused ultrasound—potential for cancer treatment. Br J Radiol 1995;68:1296–303.
14. Hutchinson EB, Buchanan MT, Hynynen K. Design and optimization of an aperiodic ultrasound phased array for intracavitary prostate thermal therapies. Med Phys 1996;23:767–76.
15. Jin CB, Wu F, Wang ZB, et al. High intensity focused ultrasound therapy combined with transcatheter arterial chemoembolization for advanced hepatocellular carcinoma. Zhonghua Zhong Liu Za Zhi 2003;25:401–3.
16. Kennedy JE, Wu F, ter Haar GR, et al. High-intensity focused ultrasound for the treatment of liver tumours. Ultrasonics 2004;42:931–5.

17. Rowland IJ, Rivens I, Chen L, et al. MRI study of hepatic tumours following high intensity focused ultrasound surgery. Br J Radiol 1997;70:144–53.

18. Wang ZB. Clinical application of high-intensity foused ultrasound in obstetrics and gynecology. Zhonghua Fu Chan Ke Za Zhi 2003;38:510–2.

19. Watkin NA, Morris SB, Rivens IH, et al. A feasibility study for the non-invasive treatment of superficial bladder tumours with focused ultrasound. Br J Urol 1996;78:715–21.

20. Wu F, Wang ZB, Chen WZ, et al. Preliminary experience using high intensity focused ultrasound for the treatment of patients with advanced stage renal malignancy. J Urol 2003;170:2237–40.

21. Van Leenders GJ, Beerlage HP, Ruijter ET, et al. Histopathological changes associated with high intensity focused ultrasound (HIFU) treatment for localised adenocarcinoma of the prostate. J Clin Pathol 2000;53:391–4.

22. Rabkin BA, Zderic V, Vaezy S. Hyperecho in ultrasound images of HIFU therapy: involvement of cavitation. Ultrasound Med Biol 2005;31:947–56.

23. Mast TD, Makin IR, Faidi W, et al. Bulk ablation of soft tissue with intense ultrasound: modeling and experiments. J Acoust Soc Am 2005;118:2715–24.

24. Cheung AY, Neyzari A. Deep local hyperthermia for cancer therapy: external electromagnetic and ultrasound techniques. Cancer Res 1984;44:4736s–44s.

25. Lele PP. Induction of deep, local hyperthermia by ultrasound and electromagnetic fields: problems and choices. Radiat Environ Biophys 1980;17:205–17.

26. Van Leenders GJ, Beerlage HP, Ruijter ET, et al. Histopathological changes associated with high intensity focused ultrasound (HIFU) treatment for localised adenocarcinoma of the prostate. J Clin Pathol 2000;53:391–4.

27. Orringer JS, Voorhees JJ, Hamilton T, et al. Dermal matrix remodeling after nonablative laser therapy. J Am Acad Dermatol 2005;53:775–82.

28. Wu F, Wang ZB, Cao YD, et al. Changes in biologic characteristics of breast cancer treated with high-intensity focused ultrasound. Ultrasound Med Biol 2003;29:1487–92.

29. Neumann RA, Knobler RM, Pieczkowski F, Gebhart W. Enzyme histochemical analysis of cell viability after argon laser-induced coagulation necrosis of the skin. J Am Acad Dermatol 1991;25:991–8.

30. Hasegawa T, Matsuzawa K, Inoue N.J. A new expansion for the velocity potential of a circular concave piston. Acoust Soc Am 1986;79:927.

31. Nyborg WL. Heat generation by ultrasound in a relaxing medium. J.Acoust Soc Amer 1981;70:310–2.

32. Makin IRS, Mast TDM, Faidi WF, et al. Miniaturized arrays for interstitial ablation and imaging. Ultrasound Med Biol 2005;31:1539–50.

33. Lin SJ, Hsiao CY, Sun Y, et al. Monitoring the thermally induced structural transitions of ollagen by use of second-harmonic generation microscopy. Opt Lett 2005;30:622–4.

34. Worthington AE, Trachtenberg J, Sherar MD. Ultrasound properties of human prostate tissue during heating. Ultrasound Med Biol 2002;28:1311–8.

35. Fry FJ, Kossoff G, Eggleton RC, Dunn F. Threshold ultrasonic dosages for structural changes in the mammalian brain. J Acoust Soc Am 1970;48(Suppl 2):1413 + .

36. Goss SA, Frizzell LA, Dunn F. Frequency dependence of ultrasonic absorption in mammalian testis. J Acoust Soc Am 1978;63:1226–9.

37. Goss SA, Johnston RL, Dunn F. Comprehensive compilation of empirical ultrasonic properties of mammalian tissues. J Acoust Soc Am 1978;64:423–57.

38. Guthkelch AN, Carter LP, Cassady JR, et al. Treatment of malignant brain tumors with focused ultrasound hyperthermia and radiation: results of a phase I trial. J Neurooncol 1991;10:271–84.

39. Yang R, Reilly CR, Rescorla FJ, et al. High-intensity focused ultrasound in the treatment of experimental liver cancer. Arch Surg 1991;126:1002; discussion 1009–10.

40. Sedelaar JP, Aarnink RG, van Leenders GJ, et al. The application of three-dimensional contrast-enhanced ultrasound to measure volume of affected tissue after HIFU treatment for localized prostate cancer. Eur Urol 2000;37:559–68.

41. ter Haar G, Sinnett D, Rivens I. High intensity focused ultrasound —a surgical technique for the treatment of discrete liver tumours. Phys Med Biol 1989;34:1743–50.

42. Chen L, Rivens I, ter Haar G, et al. Histological changes in rat liver tumours treated with high-intensity focused ultrasound. Ultrasound Med Biol 1993;19:67–74.

43. Bush NL, Rivens I, ter Haar GR, Bamber JC. Acoustic properties of lesions generated with an ultrasound therapy system. Ultrasound Med Biol 1993;19:789–801.

44. Billard BE, Hynynen K, Roemer RB. Effects of physical parameters on high temperature ultrasound hyperthermia. Ultrasound Med Biol 1990;16:409–20.

45. Damianou CA, Sanghvi NT, Fry FJ, Maass-Moreno R. Dependence of ultrasonic attenuation and absorption in dog soft tissues on temperature and thermal dose. J Acoust Soc Am 1997;102:628–34.

46. Keshavarzi A, Vaezy S, Kaczkowski PJ, et al. Attenuation coefficient and sound speed in human myometrium and uterine fibroid tumors. J Ultrasound Med 2001;20:473–80.

47. Manstein D, Herron GS, Sink RK, et al. Fractional photothermolysis: a new concept for cutaneous remodeling using microscopic patterns of thermal injury. Lasers Surg Med 2004;34:426–38.

48. Vaezy S, Andrew M, Kaczkowski P, Crum L. Image-guided acoustic therapy. Annual Rev Biomed Eng 2001;3:375–90.

Address correspondence and reprint requests to: Hans-Joachim Laubach, MD, Massachusetts General Hospital, Wellman Center for Photomedicine, BAR #305, 50 Blossom Street, Boston, MA 02114, or e-mail: hlaubach@partners.org